Z. Kristallogr. **219** (2004) 12–19
© by Oldenbourg Wissenschaftsverlag, München

TexPat – a program for quantitative analysis of oblique texture electron diffraction patterns

Peter Oleynikov*, [I], Sven Hovmöller[I], Xiaodong Zou[I], Anatoliy P. Zhukhlistov[II], Maxim S. Nickolsky[II] and Boris B. Zvyagin[II] (deceased)

[I] Stockholm University, Structural Chemistry, SE – 106 91 Stockholm, Sweden
[II] Institute of Geology of Ore Deposits, Petrography, Mineralogy and Geochemistry, Russian Academy of Sciences, Staromonetny per. 35, 109017 Moscow, Russia

Received June 5, 2003; accepted September 26, 2003

Texture patterns / Electron diffraction / intensities extraction / Program TexPat

Abstract. We have developed a program – TexPat for quantification of texture patterns in order to facilitate, speed up and improve the accuracy of this analytical method. The program introduces new approaches for automated detection of centre and symmetry axes and simplifies the process of indexing and calculating the unit cell parameters. The main algorithm of the program uses the symmetry properties of the texture pattern images. The successive steps help to process the reflections of the pattern using the peak shape extracted from well-separated peaks. The program generates a list of unit cell parameters, all processed reflections with Miller indices and their integrated intensities. The quality of the results obtained by TexPat is compatible with published data.

Introduction

Many compounds, including clay minerals, form needle- or plate-shaped crystals. Specimens of fine-grained lamellar and fiber minerals prepared by sedimentation from suspensions onto supporting surfaces or films form textures in which the component microcrystals have a preferred orientation. Texture patterns of lamellar crystals tilted with respect to the electron beam are called oblique texture electron diffraction patterns [1]. One great advantage with oblique texture patterns is that they can provide data from the full 3D diffraction pattern in a single exposure.

With finely dispersed minerals, the electron diffraction method can give a special kind of diffraction pattern, the texture pattern, which contains a two dimensional distribution of a regularly arranged set of 3D reflections [2]. Experimental data show that, owing to the small crystal dimensions, the scattering of electrons by texture specimens is in most cases quite close to kinematical ([1], [3]) which makes it easier to calculate structure factors from the integrated intensities. However, quite complicated algorithms are needed for extracting the data from texture patterns.

The analysis of texture patterns must be performed in a different way compared to regular electron diffraction patterns, due to different geometrical settings. In the first step, the centre of the texture pattern must be obtained and a background correction performed. Secondly, the main symmetry axes, which pass through the centre of the texture pattern, must be detected since the plate can be arbitrarily rotated during the digitization procedure. The last steps have the same aim as in electron diffraction structure analysis: determination of unit cell parameters and integration of intensities of indexed reflections. None of the steps in the analysis are trivial. The present work is aimed at facilitating and speeding up this analysis, using a computer program. The set of algorithms presented in this work is general and works on all types of patterns with 2*mm* symmetry.

Materials and methods

Texture patterns were taken at the Institute for Geology of Ore Deposits, Petrography, Mineralogy and Geochemistry in Moscow using a 400 kV electron diffraction camera and recorded on glass plates or imaging plates (DITABIS, Germany). Glass plates were digitized off-line using a Kite CCD camera (Calidris, Sollentuna, Sweden) with a 12-bit grey scale. Each scan produced a digital image with a size of 1280×1024 pixels. The images were saved in tiff format since it allows storing the data in 16-bit grey scale. Imaging plates were scanned by DITABIS imaging plates scanner.

All the algorithms were written using C++ programming language (Microsoft Visual C++® 6.0). All image-processing routines were implemented in a separate module library. This library has over 50 different functions to perform computations such as Fourier transforms, filtering etc. The library provides the possibility to load and save images and scaled magnitudes of the Fourier transform in several graphical formats. Another part of the program is a mathematic kernel, which provides a set of functions for

* Correspondence author (e-mail: oleyniko@fos.su.se)

working with numeric data sets: non-linear fitting, smoothing and solving systems of linear equations. The rest of the algorithms, such as indexation, unit cell parameters refinement, peak search and peak integration, were implemented in a separate module.

The developed user interface enables all the interactive operations, options and calculations to be performed via dialogs, buttons and menus. Each step can be customized. Patterns can be displayed in grey scale or transformed to pseudocolor. The user can change the color palette manually. Processed data can be saved in a special file so the user can store and load all processed information for each texture pattern. This is important because it can take a lot of time to analyze the geometry of a texture pattern in order to index the pattern and extract the intensities. The output of the program can be saved in formats, which can be read directly into standard programs used for crystal structure solution (e.g. Sir2000, SHELX-96). Another advantage of the user interface is its easy-to-follow structure: the user will not be lost in all the menus and toolbars available in the program.

Geometry of the texture patterns

The reciprocal lattice of a single crystal is a 3D set of periodic points. If a specimen contains a number of crystals then their reciprocal lattices are combined into a single reciprocal lattice with a common origin. If a specimen consists of numerous crystals of the same compound rotated at random around a certain axis, each reciprocal lattice point will generate a ring (excluding those lying on the axis of rotation) and all the rings lie on coaxial cylinders (Fig. 1a and 1b). Such a specimen is called textured and the rotation axis is called the texture axis. Since the electron wavelength is so extremely short (for example, 0.0197 Å for 300 kV) the Ewald sphere is so large that it can be approximated as a plane out to 1 Å resolution. An electron diffraction pattern is an approximate representation of a plane cross section through the reciprocal lattice passing through the common origin, perpendicular to the electron beam. When a plate texture specimen is perpendicular to the electron beam, the diffraction pattern becomes a set of concentric rings (inset in Fig. 1a).

A tilting of the texture support plane with respect to the electron beam by a tilt angle φ corresponds to cutting out a section through cylinders by a plane (Fig. 1c). This intersection gives a set of ellipses, along which the reflections are grouped (Fig. 1d).

The crystals of a texture are not perfectly parallel to the support film, but are slightly misoriented over a certain solid angular interval. Typically, the misorientation ω is about 2–4°. The smaller this interval, the more perfect is the texture. This type of distribution transforms the rings in reciprocal space to spherical bands having the common centre in the reciprocal lattice origin. As a result, the reflections on texture patterns have the shapes of arcs (Fig. 1d). A texture pattern always has 2*mm* symmetry due to its geometry (Fig. 1d).

The above mentioned geometry is only for textures rotated around one of the crystallographic axes (this is most

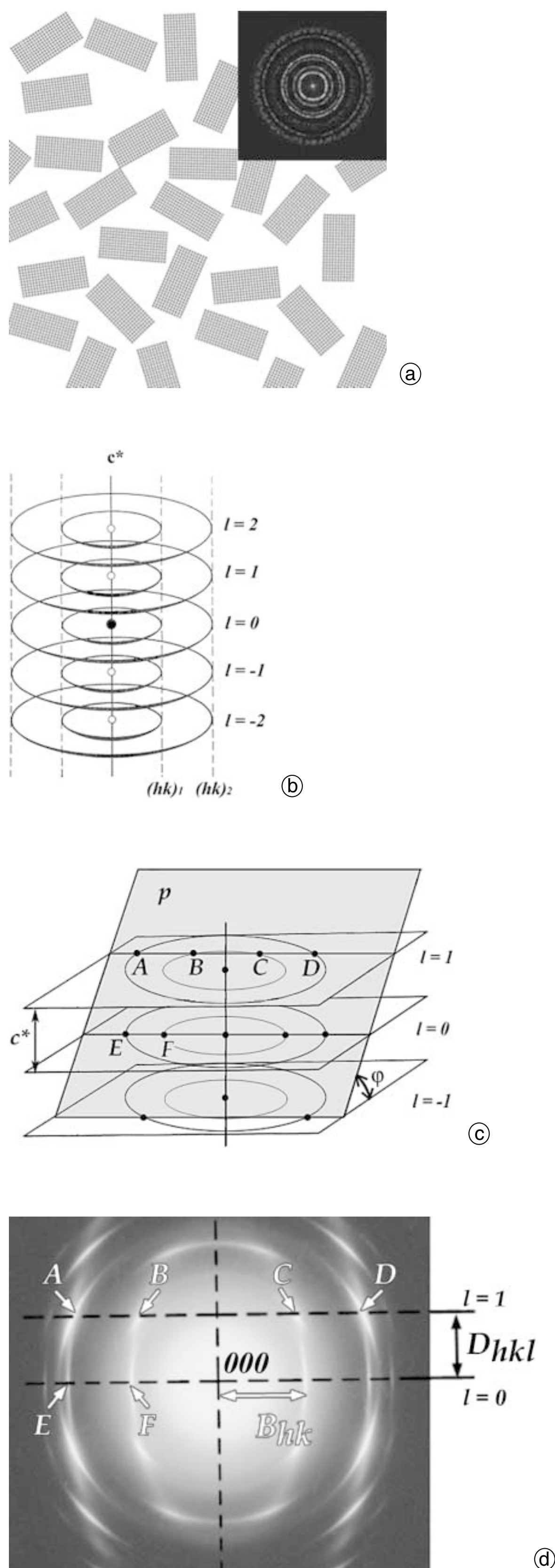

Fig. 1. Formation of a texture pattern. (**a**) A texture pattern arises from many randomly rotated flat single crystals. Inset: the Fourier transform of (a) presents a set of concentric rings. (**b**) The full 3D diffraction pattern of the texture sample is composed of several sets of rings, each with its *l* index. (**c**) An oblique texture pattern, formed by tilting the sample, is a plane *p* through the 3D diffraction pattern shown in (b). The plane *p* cuts through the diffraction pattern at points A–F. (**d**) An oblique texture pattern of lizardite. The diffraction points marked A to F correspond to those shown in (c).

easily achievable for plate-like crystals). The rotation axis (the texture axis) is defined as the c^*-axis. TexPat works only for such texture patterns.

Processing of a texture pattern by TexPat

The processing of the texture pattern by TexPat contains the following steps:

- detection of the centre;
- estimation and subtraction of the background;
- determination of the ellipse axes and the tilt angle;
- indexing and calculation of the unit cell parameters;
- integrating intensities of reflections.

Detection of the centre

The first critical step in the analysis of any texture pattern is to determine the position of the centre (*000* reflection), since all the other steps are dependent on a correctly placed centre. The centre can be positioned automatically or manually.

The automatic centre detection algorithm is based on the normalized cross-correlation [4]. Since any texture pattern has a centre of symmetry at the *000* reflection, the texture pattern remains the same when rotated by 180° around the axis perpendicular to it and passing through the *000* reflection. If the pattern is rotated around an axis passing through any position other than the *000* reflection, the resulting texture pattern will be shifted compared to the original one. This shift can be used to calculate the centre of the texture pattern, i.e. the position of the *000* reflection. This is a quite stable and accurate method for centre of symmetry detection.

Alternatively, the user can choose four symmetrically related reflections, with the same d-value, to determine the centre from those points. Then the centre of the texture pattern is at the centre of the circle containing those four reflections.

The difference between automatically calculated centre position and the centre calculated from the user-defined four reflections was found to be less then $^1/_2$ pixel in each x- and y-directions on the texture pattern with the size of 1024×1280 pixels.

Estimation and subtraction of the background

Since the background of the texture pattern is in general a radially symmetrical function, a two-dimensional background can be reconstructed from the averaged one-dimensional profile taken from the centre of the texture pattern (Fig. 2a) and then subtracted from the base image. The reflections are better resolved after background subtraction (Fig. 2b) and can be displayed in the same range of intensities. The one-dimensional profile was approximated with a Gaussian or Lorentzian function in TexPat (Fig. 2c). The user can modify control points of the approximating curve.

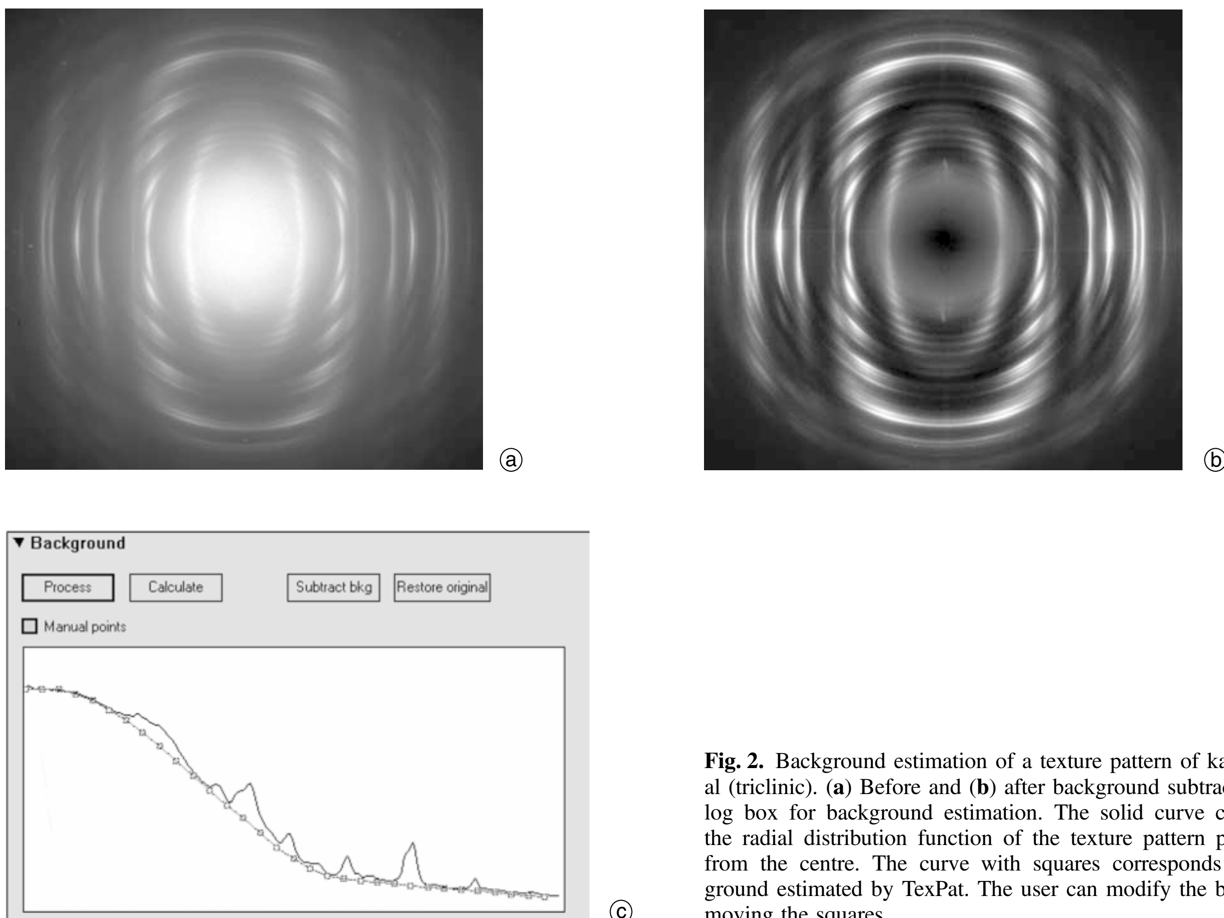

Fig. 2. Background estimation of a texture pattern of kaolinite mineral (triclinic). (**a**) Before and (**b**) after background subtraction. (**c**) Dialog box for background estimation. The solid curve corresponds to the radial distribution function of the texture pattern profile starting from the centre. The curve with squares corresponds to the background estimated by TexPat. The user can modify the background by moving the squares.

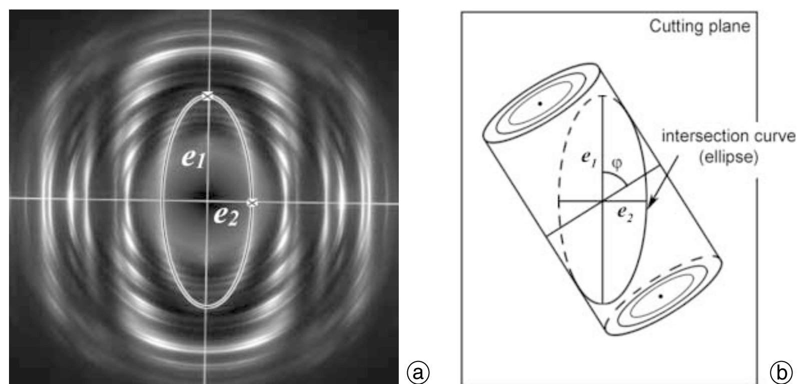

Fig. 3. Formation of ellipses of the texture patterns. (**a**) Defining the ellipse in the program by the user. (**b**) The geometry of the texture pattern.

Determination of the ellipse axes and tilt angle

In order to describe the geometry of a texture pattern, the directions of the main axes for ellipses must be found first. Since any texture pattern always contains two perpendicular mirror symmetry planes, horizontal flipping of the texture pattern helps to detect the symmetry elements of the pattern. The axes are always perpendicular to each other, so it is sufficient to find only one of those directions.

Unlike spot diffraction patterns, the reflections on a texture pattern are arcs and it is not easy to determine the centre of an arc visually. Consequently, the symmetry axes are also difficult to determine. TexPat introduces a special algorithm for determining the symmetry axes (Fig. 3a). The algorithm utilizes the $2mm$ symmetry property of the texture pattern and compares the original pattern with the horizontally flipped pattern. The flipped pattern should fit perfectly on the original pattern after a certain shift and rotation are applied. Then the rotation will tell us the direction of the mirror axes.

TexPat compares the Fourier transforms of the original and flipped texture patterns. The comparison is done in a polar coordinate system, where an angular rotation becomes a circular shift. Normalized cross correlation is used to find the value of rotation angle α of a texture pattern in order to fit the flipped pattern. The direction of the mirror axis is then half of the rotation angle α from the horizontal axis (x)

$$\beta = \alpha/2 \tag{1}$$

Fig. 3a shows the texture pattern of the mineral kaolinite with calculated main axes of symmetry marked.

The algorithm was tested on both texture patterns and spot patterns with $2mm$ symmetry and worked very well on both. The error is larger for texture patterns and increases when reflections have big azimuthal length, and can be up to 0.5° (the arc length is approximately 5 pixels at a distance of 500 pixels away from the texture pattern centre). In this case the user can choose the direction of the minor axis by picking a point, which lies on that axis. Most texture patterns have some reflections lying on that axis, simplifying the task of picking a point.

The diffraction spots in oblique texture patterns fall on sets of ellipses due to the geometry of the texture patterns (Fig. 3a). The ratio between the major and minor ellipse axes is determined by the tilt angle of the texture support plane from the plane normal to the electron beam (Fig. 3b). The tilting angle φ can be calculated from:

$$\varphi = \arccos\left(e_2/e_1\right), \tag{2}$$

where e_1 and e_2 are lengths of the major and minor ellipse axes.

The user can define these lengths for any single ellipse by moving the points along the main axes for the ellipse (Fig. 3a). The error in calculations of the tilt angle can be quite high since the major axis of any given ellipse cannot be measured directly and depends on the precision in the placement of the point by the user, while the length of the minor axis of the ellipse can be calculated with high precision: there are always some reflections with $l = 0$ lying on the minor axis, so the point can be explicitly defined by the user.

Indexing and lattice determination

One advantage of texture patterns is the possibility to determine all unit cell parameters of a crystal unambiguously and index all the diffraction peaks from only a single texture pattern. In some cases, it is even possible to distinguish different crystal systems and determine the space group of the crystal from one texture pattern.

Before determining the lattice parameters, one has to define the 3D indices for a few reflections. The indexing is based on the direct relationship between the texture pattern and the reciprocal lattice. For a reflection hkl with the reciprocal lattice vector $\boldsymbol{H_{hkl}}$:

$$\boldsymbol{H_{hkl}} = h\boldsymbol{a}^* + k\boldsymbol{b}^* + l\boldsymbol{c}^* \tag{3a}$$

$$d_{hkl} = 1/|\boldsymbol{H_{hkl}}| = 1/H_{hkl} \tag{3b}$$

where $\boldsymbol{a}^*$, $\boldsymbol{b}^*$ and $\boldsymbol{c}^*$ are the basic reciprocal lattice vectors.

Indexing a texture pattern is often rather complicated, but several characteristic features facilitate the indexation.

The distance between the line where the reflection hkl is located and the minor ellipse axis is equal to the projection of the reciprocal lattice vector $\boldsymbol{H_{hkl}}$ onto the $\boldsymbol{c}^*$ axis (which is the major ellipse axis) and can be expressed as

$$D_{hkl} = \frac{L\lambda}{\sin\varphi}\left[h \cdot a^* \cdot \cos\beta^* + k \cdot b^* \cdot \cos\alpha^* + l \cdot c^*\right] \tag{4}$$

where $L\lambda$ is a scale factor of the pattern (L is the specimen-to-film distance and λ is the wavelength) and φ the tilt angle of the texture specimen.

Since all reflections with the same h and k indices (for example 122 and 123) are located on the same cylinder (Fig. 3b), the radius of the cylinder B_{hk}, which is equal to the length of the minor ellipse axis, can be expressed in terms of real unit cell parameters a, b and γ ([1])

$$B_{hk} = \frac{L\lambda}{\sin\gamma}\sqrt{\frac{h^2}{a^2} + \frac{k^2}{b^2} - 2 \cdot \frac{h}{a} \cdot \frac{k}{b} \cdot \cos\gamma}\,. \tag{5}$$

Note that B_{hk} is independent of the l index. It is possible to calculate the values of a, b and γ unit cell parameters automatically using a set of B_{hk} values.

All six unit cell parameters of a lattice can be obtained from these two equations (4)–(5) by measuring the D_{hkl} and B_{hk} values. Generally speaking, one needs to give Miller indices of at least three independent reflections, all with different h and k and at least one with $l \neq 0$. A full and detailed description of how to index texture patterns can be found in [1].

The equations (4) and (5) are simplified for several kinds of symmetries, as described below.

The simpliest case is when α^* and β^* both are equal to 90° (including triclinic crystals with two angles = 90° or monoclinic with the unique axis c^*). Then $\cos\alpha^* = \cos\beta^* = 0$ and (4) becomes

$$D_{hkl} = \frac{L\lambda}{\sin\varphi}\, l \cdot c^*\,. \tag{6}$$

In this case, all reflection centres are lying on equidistant parallel lines. Reflections with the same l index will lie on the same horizontal line and those with the same h and k but different l will be on the same ellipse (Fig. 4a). The distance between adjacent lines is equal to the length of the reciprocal lattice vector c^*.

The value of c^* can easily be determined from the distance between the adjacent lines using (6) and so the l index is assigned for all reflections.

A more complicated case is monoclinic crystals where the unique axis does not coincide with the texture axis c^*. If b^* is the unique monoclinic axis, α^* is 90° so $\cos\beta^* = 0$, then equation (4) becomes

$$D_{hkl} = \frac{L\lambda}{\sin\varphi}\,[h \cdot a^* \cdot \cos\alpha^* + l \cdot c^*]\,. \tag{7}$$

In this case, all reflections except those with $h = 0$ will appear pair-wise on the texture pattern (Fig. 4b and 4e). The reflection pair, hkl and $\bar{h}kl$ will appear on the same ellipse but separated from each other along the c^* axis by the distance

$$2\,\frac{L\lambda}{\sin\varphi}\,h \cdot a^* \cdot \cos\beta^*\,. \tag{8}$$

All reflection pairs with the same h indices will be separated by the same distances along the c^* axis since the

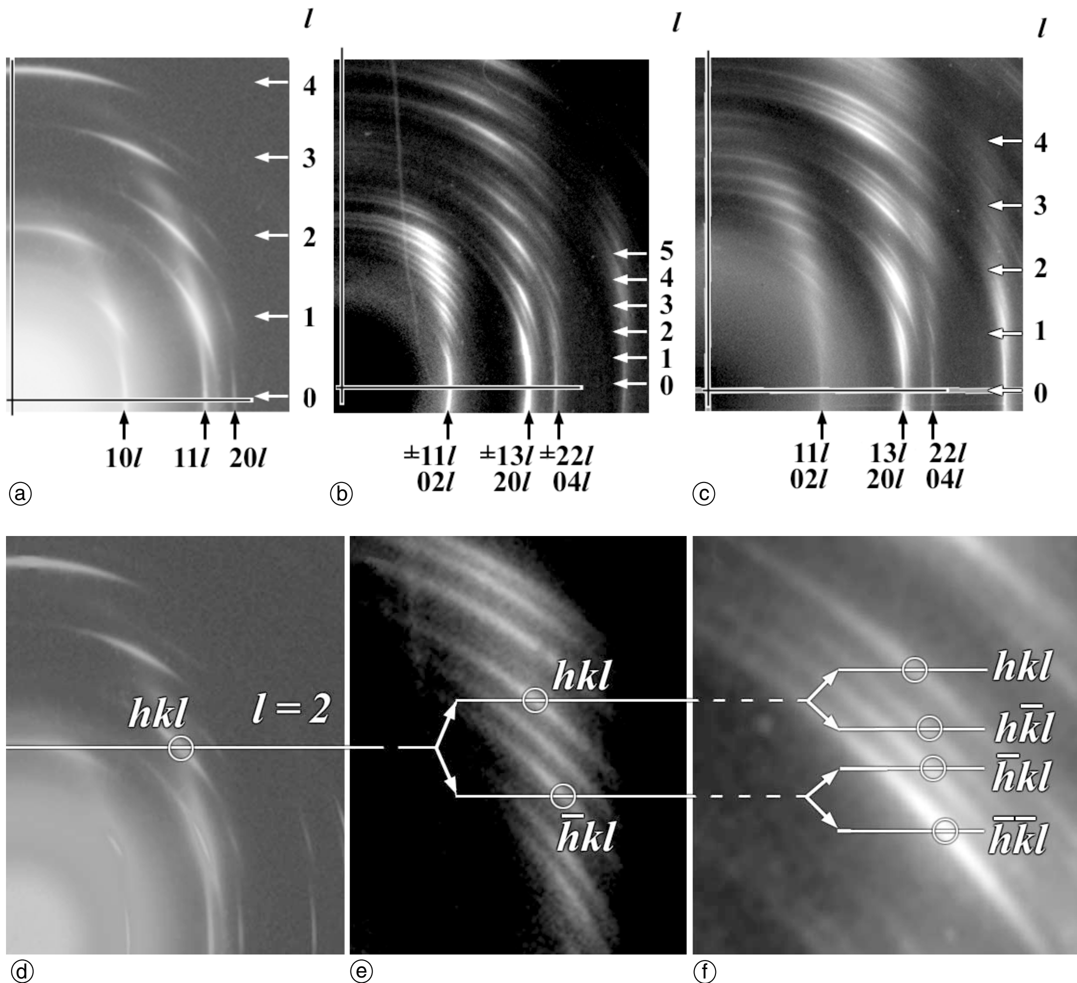

Fig. 4. Assigning the indices to the reflections (**a**) – (**c**) and splitting of the reflection hkl (**d**)–(**f**) for different symmetries. (a), (d) trigonal (lizardite 1T). (b), (e) monoclinic (muscovite $2M_1$). (c), (f) triclinic (kaolinite).

distance is proportional to the h index (Fig. 4b and 4e). The two reflections in such a pair are located with a distance of $\frac{L\lambda}{\sin\varphi}\, l \cdot c^*$ away from either side of a line that is parallel the minor axis.

Finally, for triclinic crystals with α^* and β^* both $\neq 90°$, all reflections except those with h or $k = 0$ will appear as groups of four on the texture pattern (Fig. 4c and 4f). These four reflections, hkl, $h\bar{k}l$ $\bar{h}kl$ and $\bar{h}\bar{k}l$ lie on the same ellipse, but not equally separated from each other. The reflections with the same h and k indices (within the same ellipse) will be separated in the same way along the c^* axis. The distance between the two outermost reflections, hkl and $\bar{h}\bar{k}l$, is

$$2\frac{L\cdot\lambda}{\sin\varphi}\,(h\cdot a^*\cdot\cos\beta^* + k\cdot b^*\cdot\cos\alpha^*)\,, \tag{9}$$

while the distance between the two innermost reflections, $h\bar{k}l$ and $\bar{h}kl$, is

$$2\frac{L\cdot\lambda}{\sin\varphi}\,|h\cdot a^*\cdot\cos\beta^* - k\cdot b^*\cdot\cos\alpha^*|\,. \tag{10}$$

The distance from the centre of the four reflections to the minor axis is $\frac{L\cdot\lambda}{\sin\varphi}\, l\cdot c^*$ (Fig. 4c and 4f).

In summary, reflections come in groups of four for triclinic crystals and groups of two for monoclinic crystals with the unique axis not parallel to the texture axis. In other cases all 4 reflections $\pm h \pm kl$ coincide exactly into one reflection. Then all reflections are located on equidistant lines perpendicular to the c^*.

The algorithm implemented in TexPat calculates the unit cell parameters from the three indexed reflections given by the user. Once the unit cell parameters are determined, the expected positions of all the reflections are calculated and superimposed on the texture pattern (Fig. 5a). This helps users to check if their indexing is correct. It is also possible to choose different space groups to remove forbidden reflections so the user can even check the systematic absences and determine the space group or a set of possible space groups of the crystal lattice (Fig. 5b).

The errors in the unit cell parameters determined from three reflections can be high, because the exact positions of arc-shaped reflections are difficult to define. The unit cell parameters can be further refined by TexPat, using more reflections. The user can select more, well separated reflections from the texture pattern, and then the least squares method [4] is used to minimize the differences between the experimental d-values and those calculated from the unit cell parameters. The standard deviations are also given for the refined unit cell parameters [5]. A list of theoretical reflection positions is calculated and stored for later peak splitting procedures.

Unit cell parameters (with uncertainties) calculated by TexPat, together with the earlier published data are presented in Table 1 for brucite and Table 2 for muscovite $2M_1$. They are in good agreement with published data. Here the unit cell parameters given by TexPat were scaled to the published data since the scale factor for the texture pattern was not available. The scale factor can be calculated using an internal standard, such as NaCl as an addition to the main textured sample while recording the pattern [1].

The largest error is for the c parameter of muscovite $2M_1$ which is about 1%. One reason is uncertainties in measurements of the D_{hkl} values. Another reason is the curvature of the Ewald sphere [1], which can be compensated in the next step of integrating diffraction maxima.

Integration of the diffraction maxima

The next stage is the integration of reflection intensities and the subsequent derivation of structure factors.

There are two methods for texture pattern intensity measurements described in [6]. The first approach has been used by Vainshtein, Zvyagin, Zhukhlistov and others since it can be done "by hand": integration of a small region at the centre of the arc-shaped reflection.

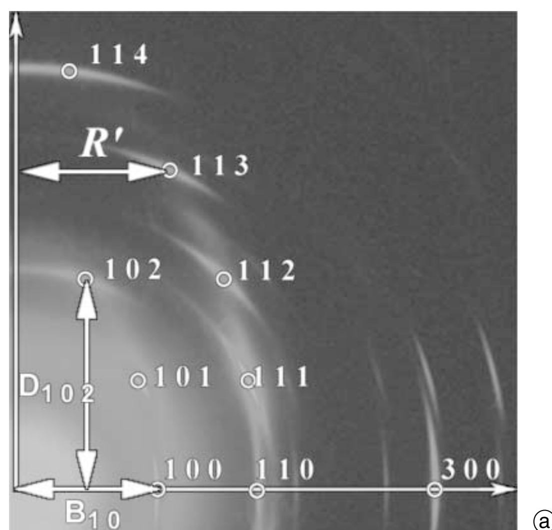

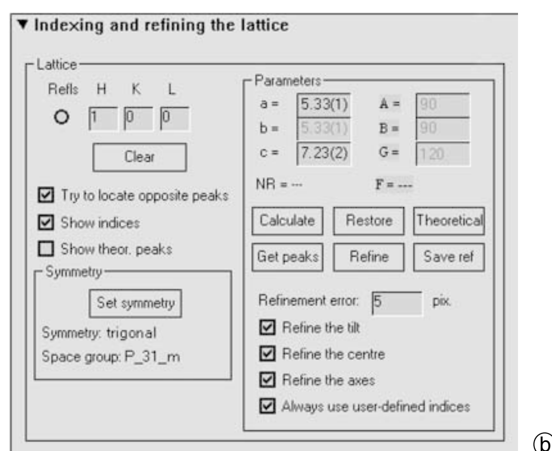

Fig. 5. (**a**) Assigning the indices for reflections for a texture pattern of lizardite-1T (space group $P31m$, $a = 5.325$ Å, $b = 7.259$ Å). All reflections on the first two ellipses are indexed with full 3D hkl indices. R' represents a horizontal position of the 113 reflection. It is important to notice the difference between B_{hk} and R' since B_{hk} is the same for all reflections with the same h and k indices (for example, reflections 100, 101 and 102 have the same $B_{hk} = B_{10}$), while R' is just a horizontal position of a reflection in the system coordinates of the texture pattern. (**b**) The dialog box which is used for indexing the texture pattern.

Table 1. Unit cell parameters for brucite (space group $P\bar{3}m1$).

Source	a/Å	c/Å
[7][a]	3.14979(4)	4.7702(7)
[8]	3.149(2)	4.769(2)
TexPat[b]	3.149(3)	4.777(4)

a: from neutron diffraction
b: scaled to the a parameter given by [8]

Then the square of the structure factor amplitude can be calculated from the "local intensity" I'_{hkl} [1], [3] as

$$|F_{hkl}|^2 \propto \frac{I'_{hkl}}{m \cdot d_{hk0} \cdot d_{hkl}}\,, \tag{11}$$

where d_{hkl} and d_{hk0} are the d values of reflection hkl and $hk0$ respectively and m is the multiplicity factor for the reflection hkl. The equation (11) uses the values of d_{hkl} and d_{hk0} in order to take into account the shape of the reflection hkl.

This approach with "local" intensities depends on the shape of the reflection and the region of integration.

The method can be used also in cases when the lengths of the arcs in an oblique texture pattern are big. In this case it is easier to measure the local intensity, for example the I'_{hkl} value in the centre of the arc.

The overlapping of peaks must be taken into account while using the approach, which is not a trivial task.

The second method is to integrate intensities under the whole arc-shaped reflections. The separation of overlapping peaks is done automatically once the peak shape has been parametrized from a few well-separated peaks. Occasionally there is a possibility of full overlapping when two or more reflections have the same or almost (within given precision) the same geometrical properties, like d and D_{hkl} values (see eqs. 3b and 4). Only then the overlapping reflections cannot be separated.

For oblique texture patterns, when the tilting angle φ is taken into account we have (in relative values):

$$|F_{hkl}|^2 \propto \frac{I_{hkl}}{m \cdot R'}\,, \tag{12}$$

Table 2. Unit cell parameters for muscovite $2M_1$ (intermediate composition of muscovite $2M_1$ and phengite $2M_1$), space group $C2/c$.

Source	a/Å	b/Å	c/Å	β/°
[9][a]	5.1906(2)	9.0080(3)	20.0470(6)	95.757(2)
[9][b]	5.2112(3)	9.0383(4)	19.9473(6)	95.769(5)
Zhukhlistov[c]	5.21	9.02	20.15	95.83
TexPat[d]	5.209(7)	9.020(9)	19.93(7)	95.6(1)

a: muscovite $2M_1$
b: phengite $2M_1$
c: manually calculated from the texture pattern, not published
d: scaled to the b parameter given by Zhukhlistov

where $|F_{hkl}|$ is the magnitude of the structure factor for the reflection hkl, R' is the distance between the reflection and the major axis of the texture pattern (shown on Fig. 5a), I_{hkl} the integrated intensity of the whole arc and m is multiplicity factor of the reflection.

It was not possible to use this method previously due to the lack of software, for estimating peak-shape parameters for all reflections simultaneously.

The peak shape was estimated from well-separated reflections by approximating the two-dimensional profile of each reflection with a 2D Gaussian or Lorentzian function. For the same texture pattern the values of full width on half maximum (FWHM) along radial and azimuthal directions varied within 5–10%. For muscovite $2M_1$ we got:

$$\mathrm{FWHM}_{\mathrm{rad}} = 5.0 \pm 0.5 \text{ pixels}\,,$$

$$\mathrm{FWHM}_{\mathrm{az}} = 21.0 \pm 1.5 \text{ pixels}\,.$$

TexPat performs integration of the intensity contained in the whole arc and gives the values of integrated intensities as well as local ones. Due to the peak overlapping, the program uses the peak shape and a list of theoretically calculated peak positions to split the pattern into non-overlapping regions. Each region may contain one reflection, non-overlapping with neighboring reflections, or more, overlapping, reflections. Data points outside these regions are not considered for further analysis.

To simplify the procedure of integration, the algorithm

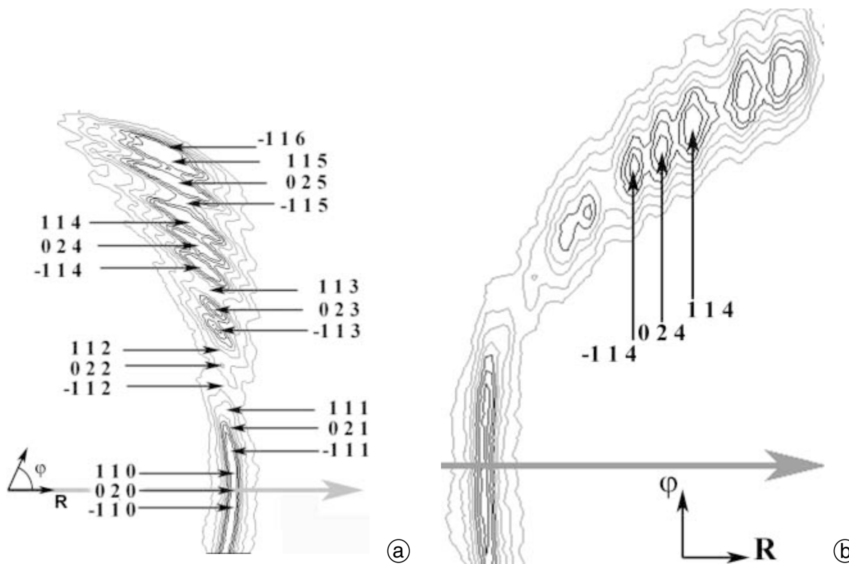

Fig. 6. Contour plots of the first ellipse for the texture pattern of the mineral muscovite $2M_1$. (**a**) Full 3D *hkl* indices marked. (**b**) Polar coordinate representation. Grey arrows represent the minor symmetry axis of the ellipse. R – radius and Φ – azimuthal angle.

Table 3. Scaled values of integrated intensities for the reflections of the brucite texture pattern.

Miller indices	I_{hkl}, [8]	I_{hkl}, TexPat	$\lvert F_{hkl}\rvert^2$, [8]	$\lvert F_{hkl}\rvert^2$, TexPat
100	1260	2384	169	340
101[a]	14700	16913	2275	2778
102[a]	11300	10208	2306	2211
110[a]	10000	9991	4031	4273
111	2000	1653	849	744
112	–	–		
113	–	–		
114	1050	739	701	524
200	–	299		171
201	2700	2020	1570	1198
202	1900	1647	1176	1082
203	800	624	567	469
204	170	125	139	108
120	–	110		110
121	1380	1054	1328	1076
122	975	900	1000	978

a: reflections which have clear dynamical influence.

performs an extra step: it converts the image of the given texture pattern (Fig. 6a) to polar coordinates (Fig. 6b).

The procedure is implemented for two-dimensional Gaussian or Lorentzian peak shape functions using the non-linear least squares fitting Levenberg-Marquardt method [4], which is specially optimized for texture patterns. Thus many variables (such as misorientation, tilt angle, radial halfwidth and unit cell parameters) can be refined simultaneously. With this algorithm all reflections can be correctly estimated – even very weak ones close to and nearly overlapped by stronger reflections, for example the weak reflection 020 (intensity 4 units) of muscovite $2M_1$ in Fig. 6a which is strongly overlapped by two neighbors – reflections 110 and -110 with intensities of 40 units each.

Any method for crystal structure determination depends on the quality of the data; unit cell parameters, Miller indices *hkl* and $|F_{hkl}|$ values for estimated reflections.

The result given in the output of the non-linear fitting procedure for the reflections taken from the imaging plate data for the texture pattern of brucite are presented in the second column of Table 3.

Reliability factors for estimated structure factors were calculated using the equation:

$$R = \frac{\sum ||F_{\text{exp}}| - |F_{\text{calc}}||}{\sum |F_{\text{exp}}|}\,. \tag{13}$$

An R-value of 7.9% was obtained in this case. This is quite accurate considering that the data comes from electron diffraction.

Conclusions

In this paper we have shown that the algorithms developed and implemented into the program TexPat may be used as a tool for accurate estimation of unit cell parameters and diffraction intensities of electron diffraction texture patterns.

The semi-automatic indexing procedure was developed to avoid manual measuring of distances within the pattern, which is very demanding, even for high symmetries, due to arc-shaped reflections.

The peak-integration procedure has the advantage of correctly estimating intensities even from patterns with severely overlapping reflections. The estimated diffraction intensities can be used for solving and refining crystal structures.

Acknowledgments. This project has been supported by the Swedish Science Research Council (VR) and Russian foundation of fundamental studies (02-05-64952). Xiaodong Zou is a Research Fellow of the Royal Swedish Academy of Sciences supported by Alice and Knut Wallenberg Foundation.

References

[1] Zvyagin, B. B.: Electron diffraction analysis of clay mineral structures. Plenum Press, New York, 1967.

[2] Zvyagin, B. B.; Zhukhlistov, A. P.; Nickolsky, M. S.: Minerals – a special area of electron diffraction structure analysis. Z. Kristallogr. **218** (2003) 316–319.

[3] Vainshtein, B. K.; Zvyagin B. B.; Avilov A. S.: Electron Diffraction Structure Analysis. In: *Electron Diffraction Techniques* (Ed. D. Dorset), vol. 1, p. 117–312. Published by IUCr 1992.

[4] Press, W. H.; Vetterling, W. T.; Teukolsky, S. A.; Flannery, B. P.: Numerical Recipes in C++, 2nd edition. Cambridge University Press 2002.

[5] Zhukhlistov, A. P.; Zvyagin, B. B.: Crystal structure of lizardite 1T based on electron diffractometer data. Kristallografiya (Rus) **43**, 6 (1998) 1009–1014.

[6] Vainshtein, B. K.: Structure analysis by electron diffraction. Pergamon Press, 1964.

[7] Catti, M.; Ferraris, G.; Hull, S.; Pavese, A.: Static compression and H disorder in brucite, $Mg(OH)_2$, to 11GPa: a powder neutron diffraction study. Phys. Chem. Minerals. **22** (1995) 200–206.

[8] Zhukhlistov, A. P.; Avilov, A. S.; Ferraris, D.; Zvyagin, B. B.; Plotnikov, V. P.: Statistical distribution of hydrogen over three positions in the brucite $Mg(OH)_2$: structure from electron diffractometry data. Crystallography Reports **42** (1997) 774–777.

[9] Güven, N.: The crystal structures of $2M_1$ phengite and $2M_1$ muscovite. Z. Kristallogr. **134** (1971) 196–212.